Supporting Information for

Manipulation of ionized impurity scattering for achieving high thermoelectric performance in n-type Mg_3Sb_2-based materials

Jun Mao[a, b⊥], Jing Shuai[a⊥], Shaowei Song[a⊥], Yixuan Wu[c], Rebecca Dally[d, e], Jiawei Zhou[f], Zihang Liu[a], Jifeng Sun[g], Qinyong Zhang[h], Clarina dela Cruz[i], Stephen Wilson[d], Yanzhong Pei[c], David J. Singh[g], Gang Chen[f], Ching-Wu Chu[a*], and Zhifeng Ren[a*]

[a] *Department of Physics and Texas Center for Superconductivity, University of Houston, Houston, TX 77204, USA*
[b] *Department of Mechanical Engineering, University of Houston, Houston, TX 77204, USA*
[c] *School of Materials Science and Engineering, Tongji University, Shanghai 201804, China*
[d] *Materials Department, University of California, Santa Barbara, California 93106, USA*
[e] *Department of Physics, Boston College, Chestnut Hill, Massachusetts 02467, USA*
[f] *Department of Mechanical Engineering, Massachusetts Institute of Technology, Cambridge, MA 02139, USA*
[g] *Department of Physics and Astronomy, University of Missouri-Columbia, Columbia, MO 65211, USA*
[h] *Key Laboratory of Fluid and Power Machinery of Ministry of Education & Center for Advanced Materials and Energy, Xihua University, Chengdu, Sichuan 610039, China*
[i] *Quantum Condensed Matter Division, Oak Ridge National Laboratory, Oak Ridge, TN 37831, USA*

⊥ These authors contributed equally to this work
*Corresponding author, email address: cwchu@uh.edu, zren@uh.edu.

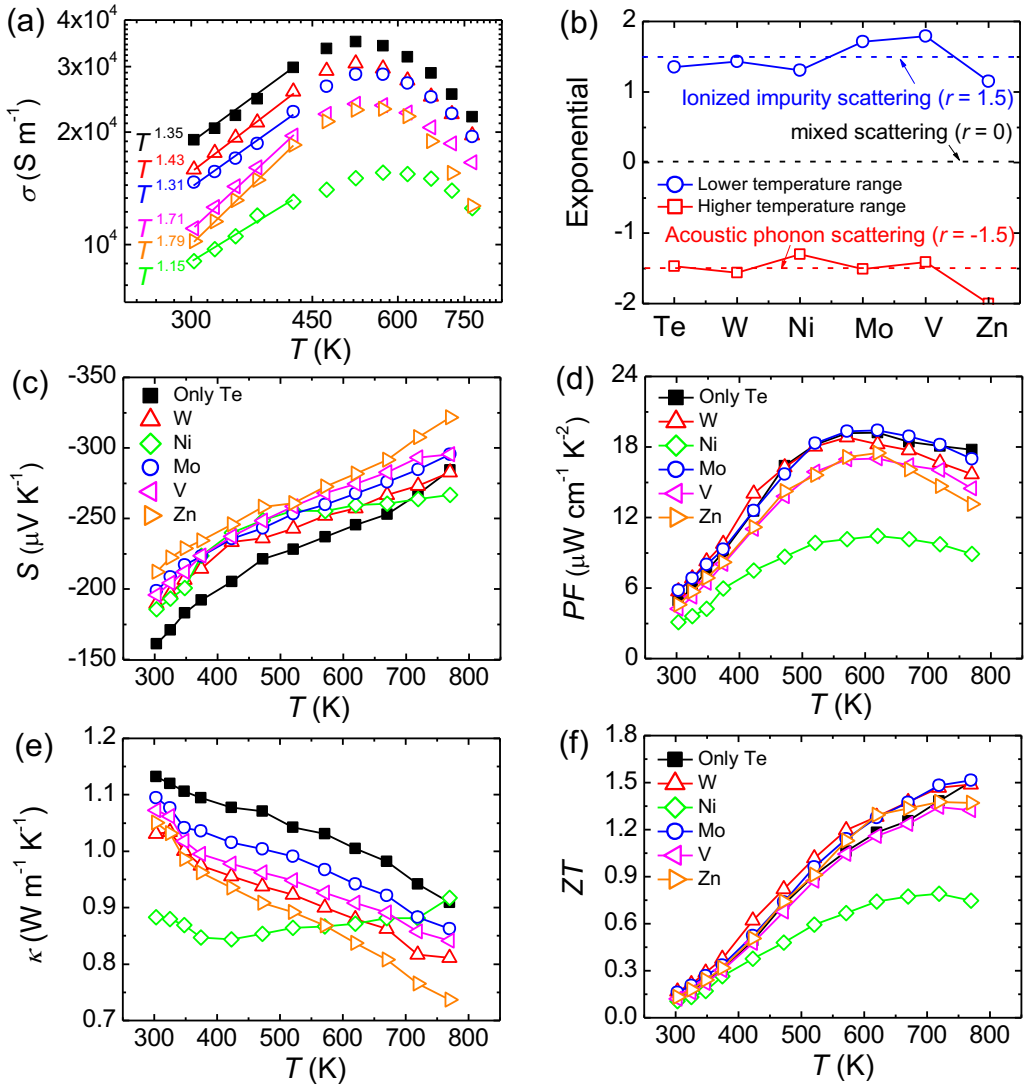

Figure S1. Thermoelectric properties of $Mg_{3.1}T_{0.1}Sb_{1.5}Bi_{0.49}Te_{0.01}$ (T = W, Ni, Mo, V, Zn). (a) Electrical conductivity, (b) temperature exponent of electrical conductivity, (c) Seebeck coefficient, (d) power factor, (e) thermal conductivity, and (f) ZT.

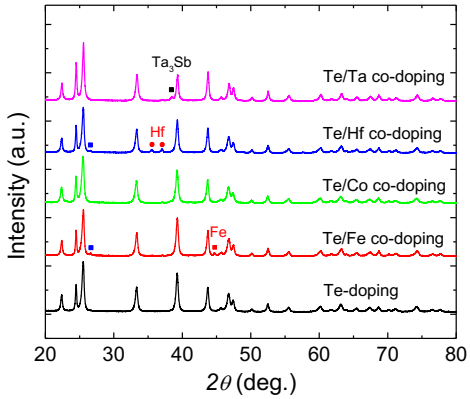

Figure S2. XRD patterns of $Mg_{3.2}A_{0.1}Sb_{1.5}Bi_{0.49}Te_{0.01}$ (A = Fe, Co, Hf, and Ta).

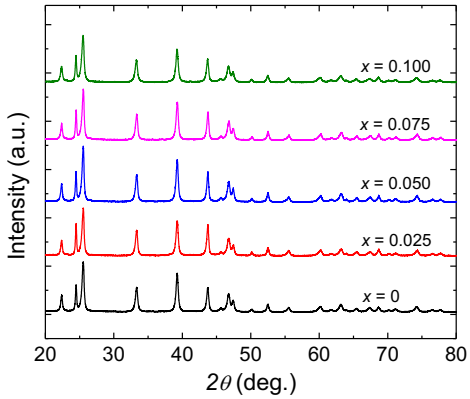

Figure S3. XRD patterns of $Mg_{3.2-x}Co_xSb_{1.5}Bi_{0.49}Te_{0.01}$ (x = 0, 0.025, 0.05, 0.075, and 0.1).

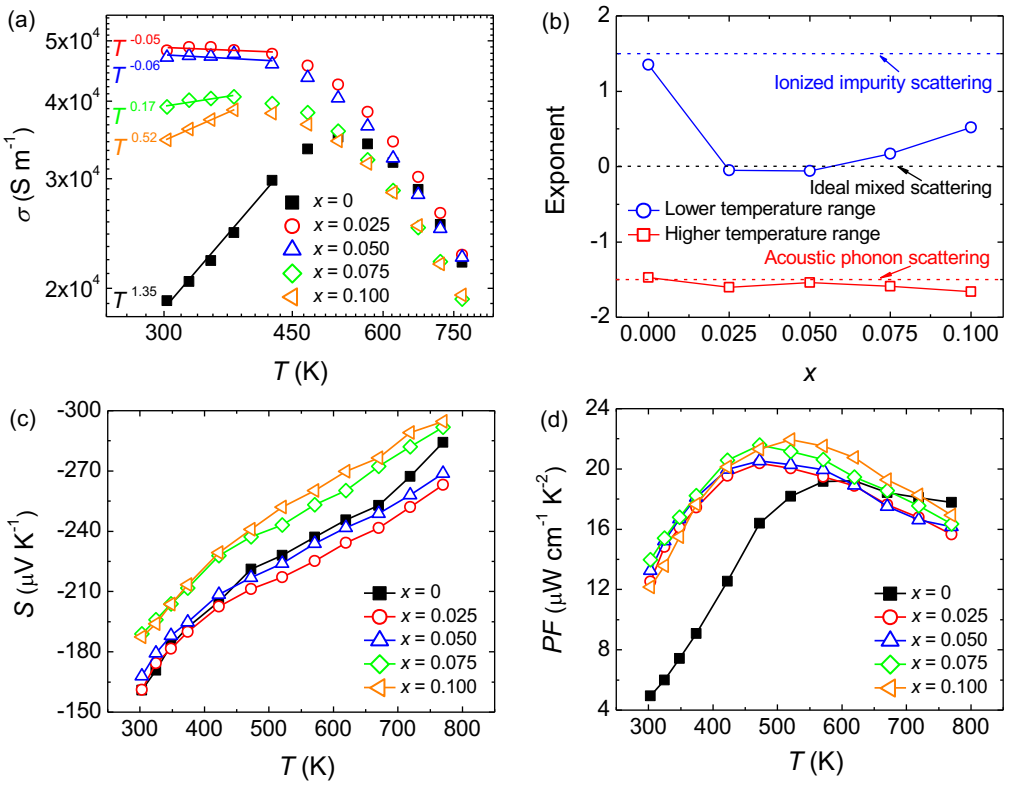

Figure S4. (a) Temperature-dependent electrical conductivity of, (b) relationship between the temperature exponent and composition for, (c) Seebeck coefficient of, and (d) *PF* of $Mg_{3.2-x}Co_xSb_{1.5}Bi_{0.49}Te_{0.01}$ (x = 0, 0.025, 0.05, 0.075, and 0.1).

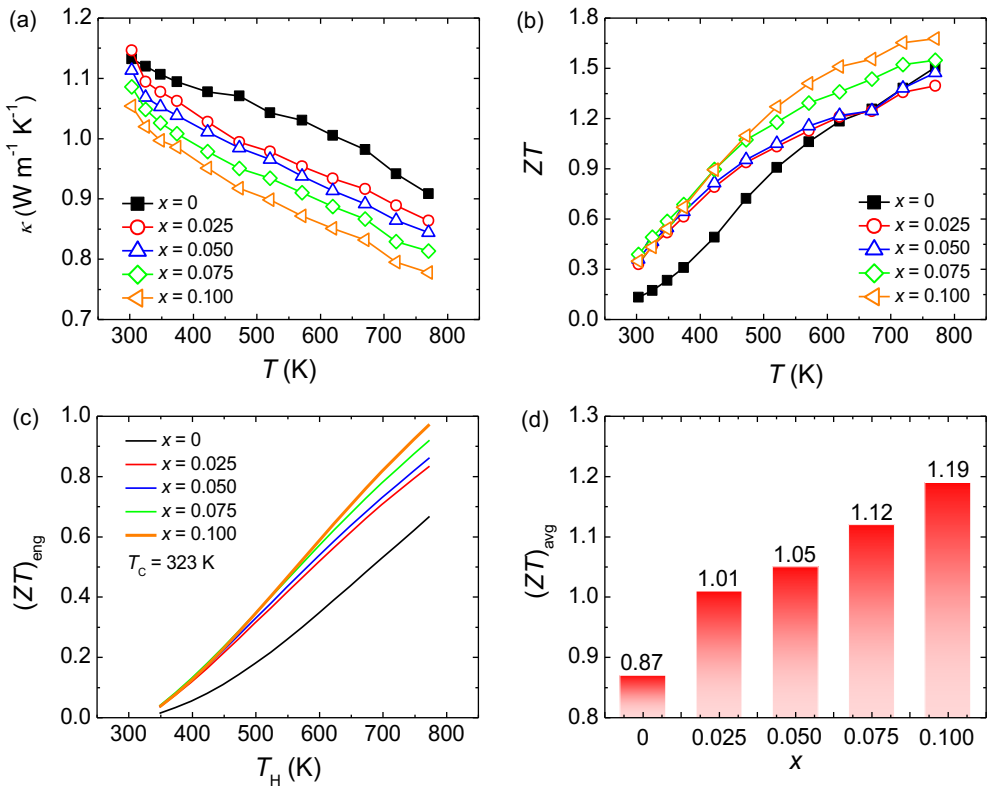

Figure S5. (a) Temperature-dependent thermal conductivity and (b) ZT of $Mg_{3.2-x}Co_xSb_{1.5}Bi_{0.49}Te_{0.01}$ (x = 0, 0.025, 0.05, 0.075, and 0.1). (c) Calculated $(ZT)_{eng}$ at T_C = 323 K and T_H = 773 K and (d) comparison of $(ZT)_{avg}$ among $Mg_{3.2}Sb_{1.5}Bi_{0.49}Te_{0.01}$ and $Mg_{3.2-x}Co_xSb_{1.5}Bi_{0.49}Te_{0.01}$.

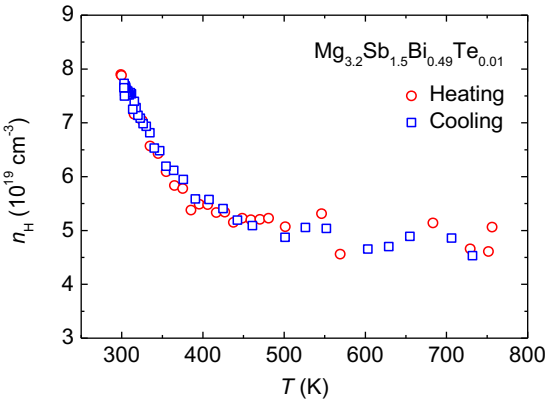

Figure S6. Repeated Hall measurements of $Mg_{3.2}Sb_{1.5}Bi_{0.49}Te_{0.01}$ during the heating and cooling cycles.

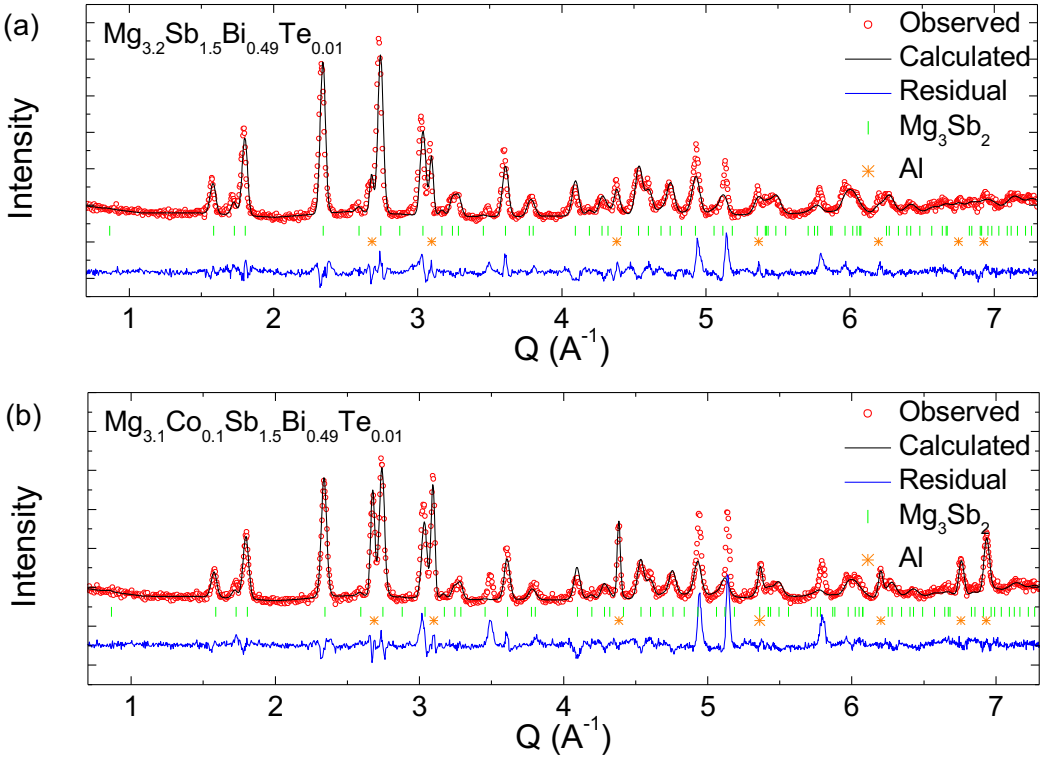

Figure S7. Rietveld refinement of neutron diffraction for (a) $Mg_{3.2}Sb_{1.5}Bi_{0.49}Te_{0.01}$ and (b) $Mg_{3.1}Co_{0.1}Sb_{1.5}Bi_{0.49}Te_{0.01}$.

The appearance of unknown impurity peaks in the samples prepared for neutron powder diffraction meant some assumptions had to be made to reach a stable, converging refinement. The first assumption made was that the Mg1 site (1/3, 2/3, z) was fully occupied for both the undoped and doped samples. This site often overfilled when refinement was attempted. The isotropic displacement parameters (B_{iso}) found

during refinement of the undoped sample were used and fixed during refinement of the doped sample. Additionally, the Co occupancy was fixed based on the formula, $Mg_{3.1}Co_{0.1}Sb_{1.5}Bi_{0.49}Te_{0.01}$. Based on the assumption that the Mg1 site was fully occupied, the Co was placed on the Mg2 site (0, 0, 0). Attempts to refine more parameters than those reported often yielded physically unreasonable values for the isotropic displacement parameters and occupations. It is possible that without the presence of impurities, a more in-depth refinement could be performed, which could yield different results.

Table S1. Detailed results for the refinement of $Mg_{3.2}Sb_{1.5}Bi_{0.49}Te_{0.01}$ and $Mg_{3.1}Co_{0.1}Sb_{1.5}Bi_{0.49}Te_{0.01}$.

	$Mg_{3.2}Sb_{1.5}Bi_{0.49}Te_{0.01}$	$Mg_{3.1}Co_{0.1}Sb_{1.5}Bi_{0.49}Te_{0.01}$
Rp	25.0	29.5
Rwp	23.9	30.1
Re	12.5	12.2
Chi2	3.684	6.106
a	4.5755(4) Å	4.5711(5) Å
c	7.2626(8) Å	7.261(1) Å
Mg1 *z*	0.6292(7)	0.6236(9)
Sb/Bi/Te *z*	0.2310(7)	0.2310(10)
B_{iso} Mg1	1.6 $Å^2$	1.6 $Å^2$
B_{iso} Mg2	1.2 $Å^2$	1.2 $Å^2$
B_{iso} Sb/Bi/Te	1.2 $Å^2$	1.2 $Å^2$
Mg2 occupation	89% ± 2%	91% ± 2%

Table S2. Calculated dielectric constant for Mg_3Sb_2 and $Mg_3Sb_{1.5}Bi_{0.5}$

Material	Contributions	*xx*	*yy*	*zz*
Mg_3Sb_2	electronic	13.8	13.8	16.4
	ionic	16.3	16.3	17.3
$Mg_3Sb_{1.5}Bi_{0.5}$	electronic	15.4	15.1	18.1
	ionic	17.3	16.9	18.1

Table S3. Densities of $Mg_{3.2}Sb_{1.5}Bi_{0.49}Te_{0.01}$ and $Mg_{3.1}A_{0.1}Sb_{1.5}Bi_{0.49}Te_{0.01}$ (A = Fe, Co, Hf, and Ta).

Specimen	Density (g cm^{-3})
$Mg_{3.2}Sb_{1.5}Bi_{0.49}Te_{0.01}$	4.41
$Mg_{3.1}Fe_{0.1}Sb_{1.5}Bi_{0.49}Te_{0.01}$	4.40
$Mg_{3.1}Co_{0.1}Sb_{1.5}Bi_{0.49}Te_{0.01}$	4.41
$Mg_{3.1}Hf_{0.1}Sb_{1.5}Bi_{0.49}Te_{0.01}$	4.54
$Mg_{3.1}Ta_{0.1}Sb_{1.5}Bi_{0.49}Te_{0.01}$	4.33

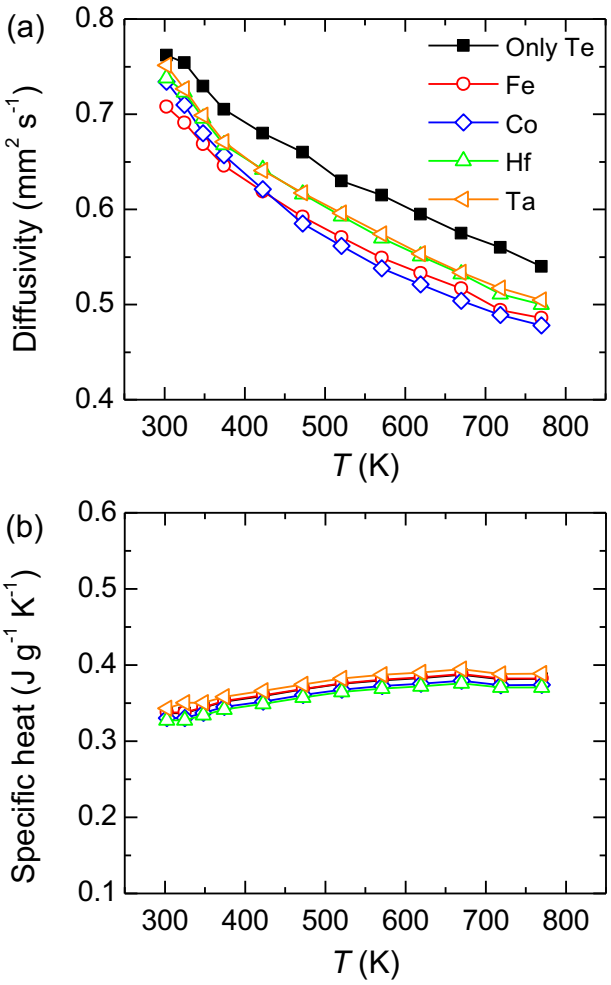

Figure S8. Thermal diffusivities and specific heat of $Mg_{3.2}Sb_{1.5}Bi_{0.49}Te_{0.01}$ and $Mg_{3.1}A_{0.1}Sb_{1.5}Bi_{0.49}Te_{0.01}$ (A = Fe, Co, Hf, and Ta).

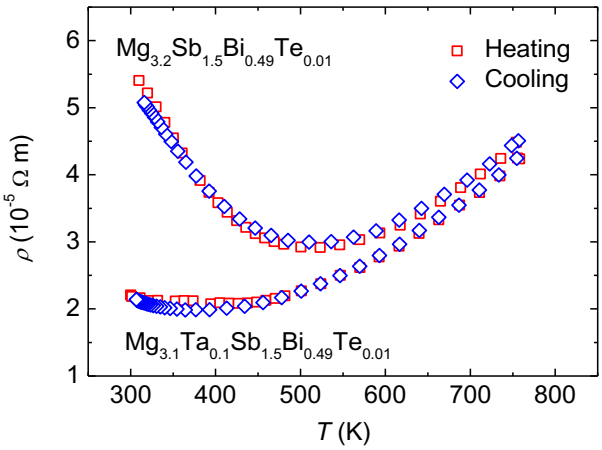

Figure S9. Electrical resistivity of $Mg_{3.2}Sb_{1.5}Bi_{0.49}Te_{0.01}$ and $Mg_{3.1}Ta_{0.1}Sb_{1.5}Bi_{0.49}Te_{0.01}$ during heating and cooling cycles.